Semicond. Sci. Technol. **22** (2007) 1086–1091 doi:10.1088/0268-1242/22/10/002

Current–voltage and noise characteristics of reverse-biased Au/n-GaAs Schottky diodes with embedded InAs quantum dots

N Arpatzanis[1], D H Tassis[1], C A Dimitriadis[1], C Charitidis[2], J D Song[3], W J Choi[3] and J I Lee[3]

[1] Department of Physics, Aristotle University of Thessaloniki, 54124 Thessaloniki, Greece
[2] School of Chemical Engineering, National Technical University of Athens, 15780 Athens, Greece
[3] Nano Device Research Center, Korea Institute of Science and Technology, Seoul 136-791, Korea

Received 27 June 2007, in final form 17 July 2007
Published 28 August 2007
Online at stacks.iop.org/SST/22/1086

Abstract
Schottky contacts on n-type GaAs with embedded InAs quantum dots (QDs) were studied by current–voltage (*I–V*) and low-frequency noise measurements. For comparison, diodes not containing QDs were investigated as reference devices. A wide distribution of the ideality factor was observed, correlated with the level of the leakage current. Reverse *I–V* characteristics on the logarithmic scale indicate that the space-charge limited current dominates the carrier transport in these diodes. In all diodes, the reverse current noise spectra show $1/f$ behaviour, attributed to traps uniformly distributed in energy within the band-gap of the GaAs capping layer. Depth profiling measurements of the $1/f$ noise power spectral density demonstrate the impact of the QDs on these traps. In diodes containing QDs, in addition to the $1/f$ noise, a generation–recombination noise is found originating from a deep trap level localized in the vicinity of the QD plane.

1. Introduction

During the last decade, great attention has been devoted to the growth and characterization of self-assembled InAs quantum dots (QDs) embedded in GaAs confining layers. Based on these materials, new generation of optoelectronic devices such as laser diodes and photodetectors is being developed [1–3]. However, due to the relatively low temperature processes involved for the growth of the QDs and GaAs capping layer, considerable non-radiative defects are induced degrading the optical properties of the structure. Among various techniques used to passivate such defects for improving the optical properties of the QDs structures, thermal annealing seems to be quite popular [4–6].

For investigation of the electronic properties of InAs QDs, extensive experimental studies were performed using Schottky diodes as test devices, the majority of which are based on the use of capacitance–voltage and deep-level transient spectroscopy (DLTS) techniques [7–9] and, more recently, low-frequency noise (LFN) measurements in the forward bias regime [10, 11]. Generally, noise measurements in forward-biased Schottky diodes can give information about the traps located within the depletion region of the junction and at the metal–semiconductor interface. In this work, our attention is focused on the electrical properties of InAs QDs embedded in GaAs by the use of current–voltage and noise measurements in reverse-biased Au/n-GaAs Schottky diodes. The variation of the noise spectral density as a function of the depletion layer width reveals the impact of the QDs on the leakage current and noise properties. Analysis of the noise data provides information for the depth distribution profile of the traps present in the GaAs confining layers. The conduction mechanism of the reverse-biased Schottky diodes is also discussed.

2. Experiments

The investigated samples were grown on silicon doped n^+ GaAs substrates in a V80 molecular beam epitaxy (MBE) system. First, a 0.4 μm thick n-type GaAs buffer layer with

the electron concentration of 1×10^{16} cm^{-3} was grown by MBE at 580 °C. Then, a 10 nm thick spacer of undoped GaAs was deposited by MBE at 480 °C, followed by a deposition by atomic layer MBE (ALMBE) of InAs with thickness equivalent to three monolayers (ML). According to the Stranski–Krastanov growth mode, InAs QDs were formed with the areal density of about 4×10^{10} cm^{-2} [10]. Finally, a 10 nm thick capping layer of undoped GaAs was deposited by MBE at 480 °C, followed by an upper GaAs layer of thickness 0.4 μm with the electron concentration of 1×10^{16} cm^{-3}. After the above growth procedures, rapid thermal annealing was performed at 700 °C for 60 s in pure nitrogen atmosphere with a 300 nm thick SiO_2 capping layer. As test devices, Schottky diodes were fabricated by thermal evaporation of Au circular dots with diameter 0.3 mm after removing the SiO_2 capping layer. A sample of the same structure, not containing InAs QDs, was prepared as a reference sample.

For electrical characterization of the diodes, the current–voltage (I–V characteristics were measured at room temperature using a computer-controlled system, including a Keithley 617 electrometer and a Keithley 230 voltage source. Noise measurements were performed at room temperature in the frequency range of 1 Hz–2 kHz in the reverse bias voltage region, using a SR760 fast Fourier transform spectrum analyser preceded by a low-noise current–voltage converter and a low-noise voltage amplifier. The diode bias was supplied by CdNi batteries to reduce any external low-frequency noise.

3. Results and discussion

Figures 1(a) and (b) show the I–V characteristics of typical Au/n-GaAs Schottky diodes for the reference samples and the structures containing InAs QDs, respectively. In the forward voltage region, the plots of log I_F versus V_F show linearity over few decades of magnitude, suggesting that thermionic-emission diffusion theory can be used to model the current in the forward regime. It is clearly shown that the leakage current is directly correlated with the ideality factor $n = (q/kT)(\mathrm{d}V_F/\mathrm{d}\ln I_F$, which can be extracted from the linear regions of the log I_F versus V_F plots. The barrier height ϕ_b, which is closely related to the ideality factor [12], was determined from the measured saturation current I_s using the relation $\phi_b = (kT/q)\ln(AA^*T^2/I_s)$, where q is the electronic charge, k is Boltzmann's constant, T is the absolute temperature, A is the diode area and A^* is Richardson's constant (8.16 A K^{-2} cm^{-2}). The average values of n and ϕ_b are 1.22 and 0.808 eV for the reference sample and 1.4 and 0.784 eV for the sample containing the QDs.

A prominent feature of figures 1(a) and (b) is the wide distribution of the I–V characteristics. The spread of the forward currents in the low-voltage region of 0–0.4 V and the reverse currents exceed three orders of magnitude. Furthermore, in comparison to the reference sample, the InAs QDs affect mainly the forward I_F–V_F characteristics in the voltage region above 0.4 V by decreasing the on-current due to the larger series resistance. A possible reason for the wide I–V distribution is that contact inhomogeneities confine the diode current to small parts of the contact areas, resulting in an effective Schottky contact area which varies from diode to diode. Such lateral barrier height inhomogeneities can arise

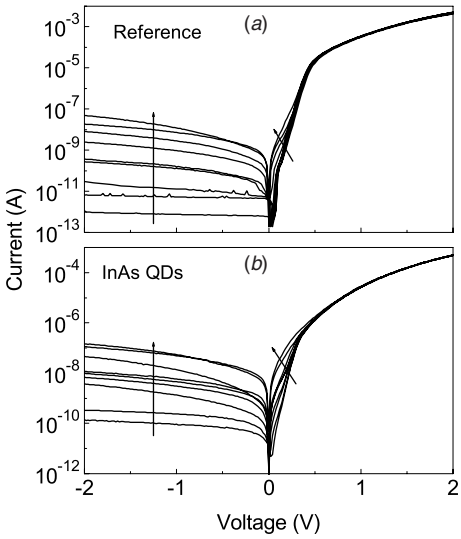

Figure 1. Current–voltage characteristics of typical Au/n-GaAs Schottky diodes fabricated on the reference samples (a) and the samples containing InAs QDs (b). The samples were subjected to post-growth thermal treatment by RTA at 700 °C for 60 s.

from atomic inhomogeneities at the metal–semiconductor interface due to grain boundaries, defects and mixture of different phases [13]. A similar wide I–V distribution has been reported in Pt/InGaAs Schottky diodes, attributed to variations in the effective Schottky contact area due to an inhomogeneous oxide and/or contaminant layer confining the current to many small regions across the contact [14].

A specific feature observed in some of the diodes on the samples with QDs is the non-exponential forward I–V behaviour, deviating from the diode characteristics which follow the thermionic-emission diffusion theory. Diodes which exhibit such non-exponential behaviour have reverse currents significantly higher than the diodes with ideality factor close to unity as shown in figure 1(b). Similar reverse current behaviour was observed in Pt/InGaAs Schottky diodes attributed to surface oxides and contaminants responsible for the formation of interface states [14]. Thus, the level of the reverse current I_r is expected to be correlated with the ideality factor n, since both are impacted by the Schottky contact quality. Figure 2 shows this correlation by plotting I_r (measured at reverse bias $V_r = 2$ V) as a function of n. About 50% of the diodes on the reference samples are near-ideal ($n < 1.1$), whereas only 10% of the diodes from those fabricated on samples with embedded QDs are near-ideal. In both types of non-ideal diodes ($n \geqslant 1.1$), one can see that I_r increases as n becomes larger. However, in diodes with the same ideality factor the reverse current is lower for the samples containing QDs, which can be attributed to an oxide layer under the Schottky contact due to a possible incomplete removal of the SiO_2 capping layer used to perform the RTA process.

In order to investigate the impact of the QDs on the reverse current, the conduction mechanism and the LFN properties of reverse-biased Schottky diodes with comparable ϕ_b and n parameters are studied. Figure 3(a) shows semilogarithmic plots of the reverse I–V characteristics of typical diodes with $n = 1.42$, $\phi_b = 0.76$ eV for the reference sample and

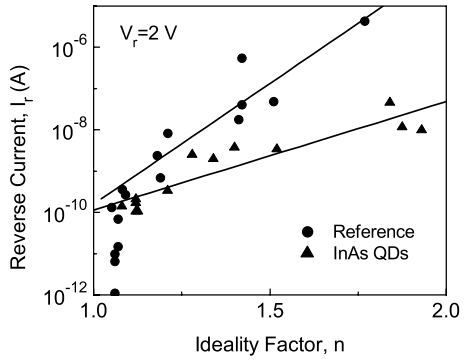

Figure 2. Plot of the reverse current versus the ideality factor for Au/n-GaAs Schottky diodes fabricated on the reference samples and the samples containing InAs QDs. The current was measured at the reverse bias of $V_r = 2$ V.

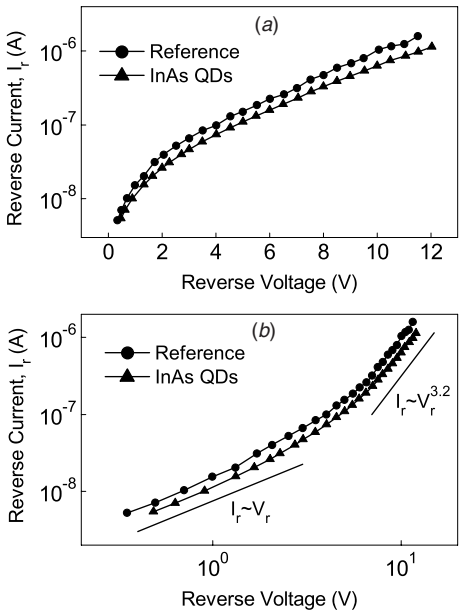

Figure 3. Semilogarithmic (*a*) and logarithmic (*b*) plots of the reverse I–V characteristics of Schottky diodes fabricated on a reference sample and a sample containing InAs QDs. The diode parameters are $n = 1.42$, $\phi_b = 0.76$ eV for the reference sample and $n = 1.47$, $\phi_b = 0.76$ eV for the sample with embedded QDs.

$n = 1.47$, $\phi_b = 0.76$ eV for the sample with embedded QDs. To clarify the reverse current conduction mechanism, the I–V characteristics of figure 3(*a*) are plotted on logarithmic scales as shown in figure 3(*b*). In both diodes, at low voltages (<2 V) an ohmic behaviour is observed, whereas at higher voltages (>6 V) the current rises quickly described by a power-law-type relationship between I_r and V_r given by $I_r \propto V_r^{3.2}$. These features in the logarithmic plots can be interpreted as arising from space-charge limited current (SCLC) conduction in the presence of single-energy deep trapping centres [15]. The slow rise in current between 2 and 6 V is indicative of a distribution of trapping states in the forbidden energy gap [16].

The trap properties of the Schottky diodes of figure 3 are investigated by employing the LFN technique. Figure 4(*a*) shows typical current noise spectra for the reference diode,

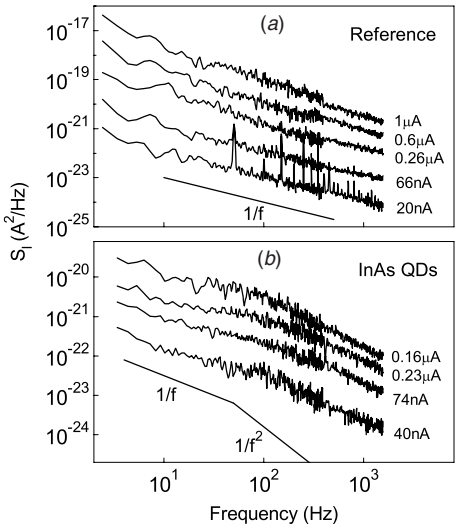

Figure 4. Typical spectral current density S_I as a function of the frequency for the Au/n-GaAs Schottky diodes fabricated on the reference sample (*a*) and the sample with InAs QDs (*b*), measured at different reverse currents.

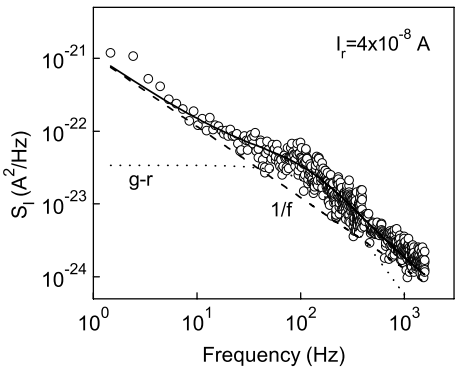

Figure 5. Decomposition into $1/f$ and g–r noise components of the spectral current density for the Au/n-GaAs Schottky diode containing InAs QDs, measured at the reverse current of 40 nA.

measured in the frequency range of 1 Hz–2 kHz at different reverse currents. In the investigated frequency range, for the reference diode the current spectral density S_I shows $1/f$ behaviour for all currents. For the diode with embedded QDs, S_I shows $1/f$ behaviour in the frequency range of 1–100 Hz, followed by the $1/f^2$ dependence at frequencies above 100 Hz as shown in figure 4(*b*). These results indicate that the noise in diodes with QDs can be treated as a linear combination of two noise sources: a $1/f$ noise component arising from distributed in energy traps and a generation–recombination (g–r) spectrum characterized by a plateau at low frequencies, followed by the $1/f^2$ dependence at higher frequencies. The existence of a g–r noise indicates the presence of a distinct trap level in the bulk of the GaAs capping layer [17].

For the diode with embedded QDs, figure 5 shows the decomposition of a typical experimental noise spectrum into $1/f$ and noise components using the relationship

$$S_I = \frac{B}{f} + C\frac{1/f_c}{1 + (f/f_c)^2}, \qquad (1)$$

where the fitting constants B and C represent the relative

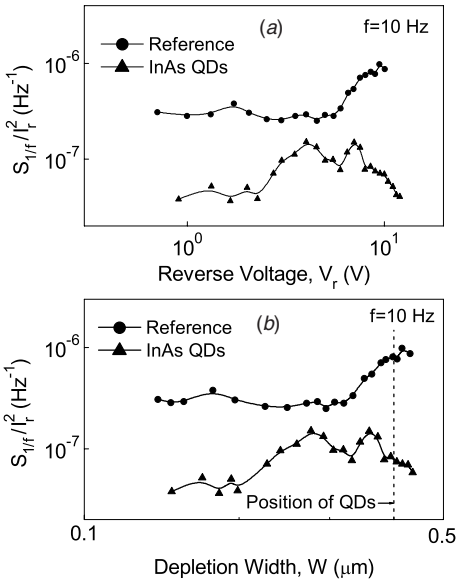

Figure 6. Normalized reverse current power spectral density $S_{1/f}/I_r^2$ as a function of the reverse voltage (*a*) and the depletion region width (*b*) for the Au/n-GaAs Schottky diodes of figure 4.

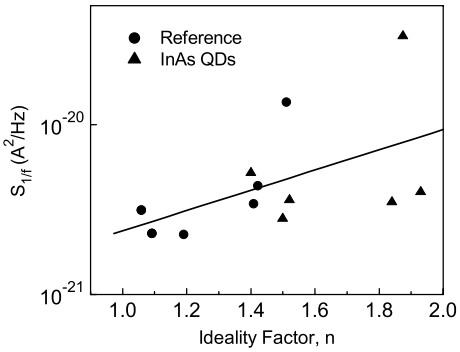

Figure 7. Spectral current density $S_{1/f}$ as a function of the ideality factor for Au/n-GaAs Schottky diodes fabricated on reference samples and samples with InAs QDs. The noise measurements were performed at the frequency of $f = 10$ Hz and the constant reverse current of 0.1 μA.

magnitude of the $1/f$ and g–r processes, respectively. f_c is the corner frequency of the g–r noise, which is related to the trap time constant by $\tau = 1/2\pi f_c$. As shown in figure 5, $1/f$ noise source and a single g–r level fit well the experimental data, with the magnitude of the $1/f$ noise exceeding the g–r noise magnitude for frequencies lower than 35 Hz.

For the reference diode and the diode with embedded QDs, plots of the normalized $1/f$ noise power spectral density $S_{1/f}/I_r^2$ as a function of the reverse bias voltage V_r are presented in figure 6(*a*). The $S_{1/f}/I_r^2$–V_r curves were converted into $S_{1/f}/I_r^2$–W curves by determining the space-charge region width W from capacitance–voltage measurements using the relation $W = \varepsilon A/C$, where ε is the dielectric permittivity of GaAs and C is the capacitance of the junction. The results of conversion (i.e. the normalized noise $S_{1/f}/I_r^2$ as a function of the depletion width W) are shown in figure 6(*b*).

From figure 6(*b*), it is seen that $S_{1/f}/I_r^2$ remains unchanged with increasing W from about 0.13 to 0.32 μm for the reference sample, i.e. the noise $S_{1/f}$ obeys the relationship $S_{1/f} \propto I_r^\alpha$ with $\alpha = 2$. The exponent $\alpha = 2$ of the $1/f$ noise current dependence indicates that traps having a constant cross-section are evenly distributed both in the space-charge region and in energy within the semiconductor band-gap [18]. For $W > 0.32$ μm, as the edge of the depletion region approaches the interface between the spacer of undoped GaAs (10 nm thick) and the doped GaAs capping layer (0.4 μm thick), $S_{1/f}/I_r^2$ increases abruptly with W. This fast increase of the $1/f$ component can be attributed to the involvement at the traps located at the interface between the spacer and capping GaAs layers. For the sample containing QDs, the depletion region width where $S_{1/f}/I_r^2$ remains unchanged is limited in the region from about 0.13 to 0.2 μm as shown in figure 6(*b*). However, for $W > 0.2$ μm as the edge of the depletion region approaches the QDs plane, two peaks of the $S_{1/f}/I_r^2$–W profile are observed located at about 0.28 and 0.36 μm from the Schottky contact. This result indicates the accumulation of energy-distributed traps at the corresponding positions, arising from the insertion of the QDs.

The spectral density $S_{1/f}$ of the $1/f$ noise and the ideality factor n are expected to be correlated, since they are impacted by the Schottky contact quality. For the GaAs Schottky diodes on the reference samples and the structures with QDs, figure 7 shows this correlation by plotting $S_{1/f}$ as a function of n, where the noise was measured at the reverse current $I_r = 0.1$ μA and frequency $f = 10$ Hz. One can see that a weak correlation between $S_{1/f}$ and n exists for the investigated Au/n-GaAs Schottky diodes. A similar correlation between $S_{1/f}$ and n was found to exist for evaporated Pt/InGaAs Schottky contacts, where the measured $1/f$ noise was attributed to recombination centres located farther away from the Schottky contact, i.e. deeper into the semiconductor [14]. A stronger correlation between $S_{1/f}$ and n was observed in plated Pt/InGaAs Schottky contacts, where the spread of I–V characteristics was significantly less compared to the evaporated Schottky contacts and the measured $1/f$ noise was attributed to recombination centres localized at the interface of the Schottky contact [14].

For the g–r noise resulting from trapping–detrapping processes between states in the conduction band and a monoenergetic trap level, the spectrum is described by the relationship

$$S_{g\text{–}r} = \frac{\tau I_r^2 A_{g\text{–}r}}{1 + (\omega\tau)^2}, \tag{2}$$

where $\omega = 2\pi f$ and $A_{g\text{–}r}$ is a unitless quantity representing the magnitude of the individual g–r process [19]. From equation (2), the intensity of the low-frequency plateau of the g–r noise spectrum is given by

$$S_{g\text{–}r}(0) = \frac{I_r^2 A_{g\text{–}r}}{f_c}. \tag{3}$$

The plot of the g–r noise intensity $S_{g\text{–}r}(0)$ as a function of the reverse current for the Schottky diode containing QDs is presented in figure 8(*a*). The solid line shows an I_r^2 variation of $S_{g\text{–}r}(0)$ as predicted by equation (3). An average value for the corner frequency of the g–r noise was found to be about $f_c = 150$ Hz as shown in the plot of figure 8(*b*). In the g–r

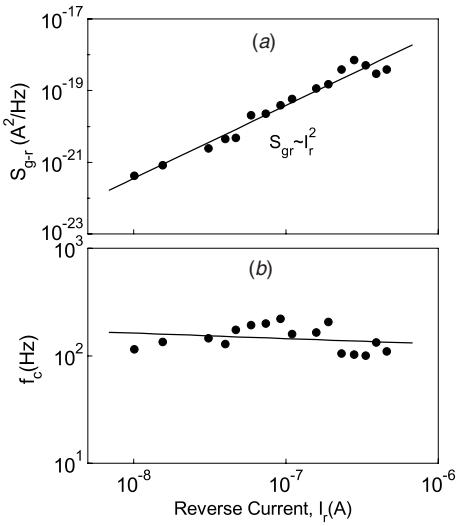

Figure 8. Spectral current density S_{g-r} (*a*) and corner frequency f_c (*b*) as a function of the reverse current obtained from analysis of the noise spectra of the Au/n-GaAs Schottky diode with embedded InAs QDs.

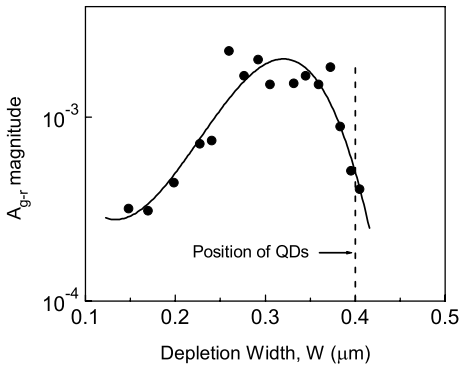

Figure 9. Variation of the g–r noise parameter A_{g-r} with the depletion region width derived from the experimental noise data of figure 8(*a*).

model, the time constant of the noise with Lorentzian spectrum is defined as

$$\tau = \tau_{act} \exp\left(\frac{\Delta E_t}{kT}\right), \tag{4}$$

where the pre-exponential parameter τ_{act} is related to phonon vibration which is of the order of 10^{-14} s [20]. Using the experimental value of $f_c = 150$ Hz, from the relation $\tau = 1/2\pi f_c$ and equation (4) we determined the activation energy of $\Delta E_t = 0.65$ eV, indicating the presence of a deep trap level located near the mid-gap of the GaAs capping layer. The S_{g-r}–I_r curve of figure 8(*b*) was converted into the A_{g-r}–W curve, which is presented in figure 9. The position of the peak of the W-shaped profile, located at about 0.32 μm from the Schottky contact, demonstrates that the deep trap level in the GaAs capping layer is accumulated at a position close to the QDs plane.

4. Conclusions

The electrical properties of Schottky contacts on n-type GaAs with embedded InAs quantum dots (QDs) were investigated by *I–V* and low-frequency noise measurements. For comparison, diodes without containing QDs were investigated as reference devices. In the diodes with or without QDs, a wide distribution of the ideality factor was observed, correlated with the level of the leakage current. The main features of the reverse *I–V* characteristics indicate that SCLC dominates the carrier transport in these diodes, influenced by the presence of a deep trap level and a distribution of trapping states in the forbidden energy gap of the GaAs capping layer.

To probe the properties of these traps in the GaAs capping layer, noise measurements were performed as a function of the reverse bias voltage. In all Schottky diodes, the reverse current noise spectra show $1/f$ behaviour, attributed to traps uniformly distributed in the forbidden energy gap of the GaAs capping layer. In the diode containing QDs, in addition to the $1/f$ noise, a g–r noise is found originating from a discrete trap level located about 0.65 eV from the conduction band edge. Depth profiling measurements of the $1/f$ and g–r noise power spectral densities indicate accumulation of the energy distributed traps and the deep trap level at positions close to the QDs plane.

Acknowledgments

The Greek authors are grateful to the Greek General Secretariat for Research and Technology for financial support under the contract 05NON-EU-174. In Korea, the work was supported by the Korea Foundation for International Cooperation of Science and Technology (KICOS) through a grant provided by the Korean Ministry of Science and Technology (MOST) (no M60605000007-06A0500-00710). One of the authors (JDS) acknowledges the partial support from SPINTRONICS KIST Institutional program.

References

[1] Campell J C, Huffaker D L and Deng H 1997 *Electron. Lett.* **33** 1337
[2] Heinrichsdorff F, Mao M H and Kirstaedter N 1997 *Appl. Phys. Lett.* **71** 22
[3] Shchekin O B and Deppe D G 2002 *Appl. Phys. Lett.* **80** 3277
[4] Sobolev M M, Koshnev I V, Lantratov V M, Bert N A, Cherkoshin N A, Ledentsov N N and Bedarev D A 2000 *Semiconductor* **34** 195
[5] Le Ru E C, Fack J and Murray R 2003 *Phys. Rev.* B **67** 245318
[6] Tatebayashi J, Arakawa Y, Hatori N, Ebe H, Sugawara M, Sudo H and Kuramata A 2004 *Appl. Phys. Lett.* **85** 1024
[7] Drexler H, Leonard D, Hansen W, Kotthaus J P and Petroff P M 1994 *Phys. Rev. Lett.* **73** 2252
[8] Chiquito A J, Pusep YuA, Mergulhao S, Galzerani J C and Moshegov N T 2000 *Phys. Rev.* B **61** 5499
[9] Wang H L, Ning D, Zhu H J, Chen F, Wang H, Wang X D and Feng S L 2000 *J. Cryst. Growth* **208** 107
[10] Song J D, Choi W J, Han I K, Lee J I, Kim J H, Song J I and Chovet A 2004 *J. Korean Phys. Soc.* **45** S542
[11] Tsormpatzoglou A, Tassis D H, Dimitriadis C A, Frigeri P, Franchi S, Gombia E and Mosca R 2006 *IEEE Electron Dev. Lett.* **27** 320
[12] Koutsouras D A, Hastas N A, Tassis D H, Dimitriadis C A, Frigeri P, Franchi S, Gombia E and Mosca R 2005 *J. Appl. Phys.* **97** 064506
[13] Sullivan J P, Tung R T, Pinto M R and Graham W R 1991 *J. Appl. Phys.* **70** 7403

[14] Marsh P, Pavlidis D and Hong K 1998 *IEEE Trans. Electron Devices* **45** 349
[15] Lampert M A and Mark P 1970 *Current Injection in Solids* (New York: Academic)
[16] Hall H P, Awaah M A and Das K 2004 *Phys. Status Solidi* **201** 522
[17] Hooge F N 1994 *IEEE Trans. Electron Devices* **41** 1926
[18] Hsu S T 1970 *IEEE Trans. Electron Devices* **17** 496
[19] Copeland J A 1971 *IEEE Trans. Electron Devices* **18** 50
[20] Dutta P and Horn P M 1981 *Rev. Mod. Phys.* **53** 497